International Journal of Bifurcation and Chaos, Vol. 22, No. 2 (2012) 1250033 (15 pages)

DOI: 10.1142/S0218127412500332

MULTI-SCROLL CHAOTIC AND HYPERCHAOTIC ATTRACTORS GENERATED FROM CHEN SYSTEM*

XINZHI LIU
Department of Applied Mathematics,
University of Waterloo, Waterloo,
Ontario N2L 3G1, Canada
xzliu@math.uwaterloo.ca

XUEMIN (SHERMAN) SHEN† and HONGTAO ZHANG‡
Department of Electric and Computer Engineering,
University of Waterloo, Waterloo,
Ontario N2L 3G1, Canada
†*xshen@bbcr.uwaterloo.ca*
‡*h15zhang@bbcr.uwaterloo.ca*

Received December 15, 2011

In this paper, we create a multi-scroll chaotic attractor from Chen system by a nonlinear feedback control. The dynamic behavior of the new chaotic attractor is analyzed. Specially, the Lyapunov spectrum and Lyapunov dimension are calculated and the bifurcation diagram is sketched. Furthermore, via changing the value of the control parameters, we can increase the number of equilibrium points and obtain a family of more complex chaotic attractors with different topological structures. By introducing time delay to the feedback control, we then generalize the multi-scroll attractor to a set of hyperchaotic attractors. Computer simulations are given to illustrate the phase portraits with different system parameters.

Keywords: Chaos; Chen system; Lyapunov exponent; Hopf bifurcation.

1. Introduction

Over the past two decades, the generation of chaotic or hyperchaotic systems and their applications have attracted a great deal of attention [Ballinger & Liu, 1997; Chen & Ueta, 1999; Cuomo & Oppenheim, 1993; Khadra *et al.*, 2003; Kocarev *et al.*, 1992; Liu, 2006; Pecora & Carroll, 1990; Yang & Chua, 1996]. Especially, multi-scroll attractors and hyperchaos systems have been intensively studied [Goedgebuer *et al.*, 1998; Grassi & Mascolo, 1999; Li & Chen, 2004; Li *et al.*, 2005; Lu *et al.*, 2004; Peng *et al.*, 1996; Rossler, 1979; Yalcin, 2007; Yan & Yu, 2008]. Recently, a nonautonomous technique to generate multi-scroll attractors and hyperchaos has been introduced [Elwakil & Ozoguz, 2006; Li *et al.*, 2005]. Using switching systems, some new chaotic attractors have been achieved in [Liu *et al.*, 2006; Lu *et al.*, 2004]. Some fractional differential systems have also been presented to generate chaos [Ahmad & Sprott, 2003; Hartley *et al.*, 1995; Li & Chen, 2004], and some simple circuits have been developed to realize chaos [Chua *et al.*, 1993; Elwakil & Kennedy, 2001; Lu *et al.*, 2004; Yalcin, 2007; Yalcin *et al.*, 2002].

*Research supported by NSERC Canada.

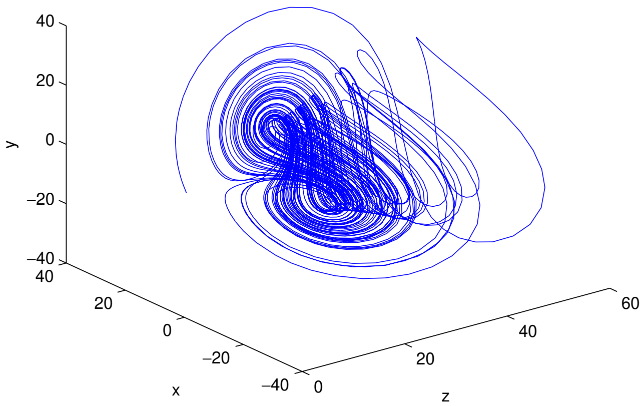

Fig. 1. The phase portrait of Chen system with $a = 35$, $b = 3$ and $c = 28$, starting with $[1, 1, 1]$.

It is well known that a first-order delay differential equation can generate chaotic and even hyperchatic attractors [Farmer, 1982; Ikeda & Matsumoto, 1987]. Since Mackey–Glass system, which is a physiological model, was found to possess chaotic behaviors, several modified chaotic systems have been reported [Lu & He, 1996; Namajunas *et al.*, 1995; Tamasevicius *et al.*, 2006; Wang & Yang, 2006]. Some experimental observations of multi-scroll attractors have been confirmed [Tamasevicius *et al.*, 2006; Wang & Yang, 2006; Yalcin & Ozoguz, 2007]. In this paper, we use feedback function to control Chen system to multi-scroll attractors, via increasing its equilibrium points. Furthermore, we introduce time delay to the control function to generalize it to more complex chaos and hyperchaos.

The remainder of this paper is organized as follows. In Sec. 2, we present a control function to generate a 6-scroll attractor from Chen system. In Sec. 3, we analyze the dynamical behavior of the new attractor. In Sec. 4, by controlling the values of system parameter, we generalize the system to different multi-scroll chaotic attractors. In Sec. 5, by introducing time delay to the control function, we achieve more complex chaos and hyperchaos. Finally, conclusions are given in Sec. 6.

2. New Chaotic Attractor

Chen system was introduced in 1999 when he studied how to control the Lorenz system. It has been proved that Chen system is not topologically equivalent to the Lorenz system. The mathematical model is given as

$$\begin{cases} \dot{x} = a(y - x), \\ \dot{y} = (c - a)x - xz + cy, \\ \dot{z} = xy - bz. \end{cases} \tag{1}$$

Figure 1 shows the phase portrait of Chen system with $a = 35$, $b = 3$ and $c = 28$.

We consider the following controlled system,

$$\begin{cases} \dot{x} = a(y - x) \\ \dot{y} = (c - a)x - xu + cy \\ \dot{z} = xy - bz \end{cases} \tag{2}$$

where the control function $u(t) = d_1 z(t) - d_2 \sin(z(t))$ with $a = 35, b = 3, c = 28$, $d_1 = 1$ and $d_2 = 8$. Figure 2 shows the phase portraits of the state variables of the controlled Chen system, which is a 6-scroll attractor.

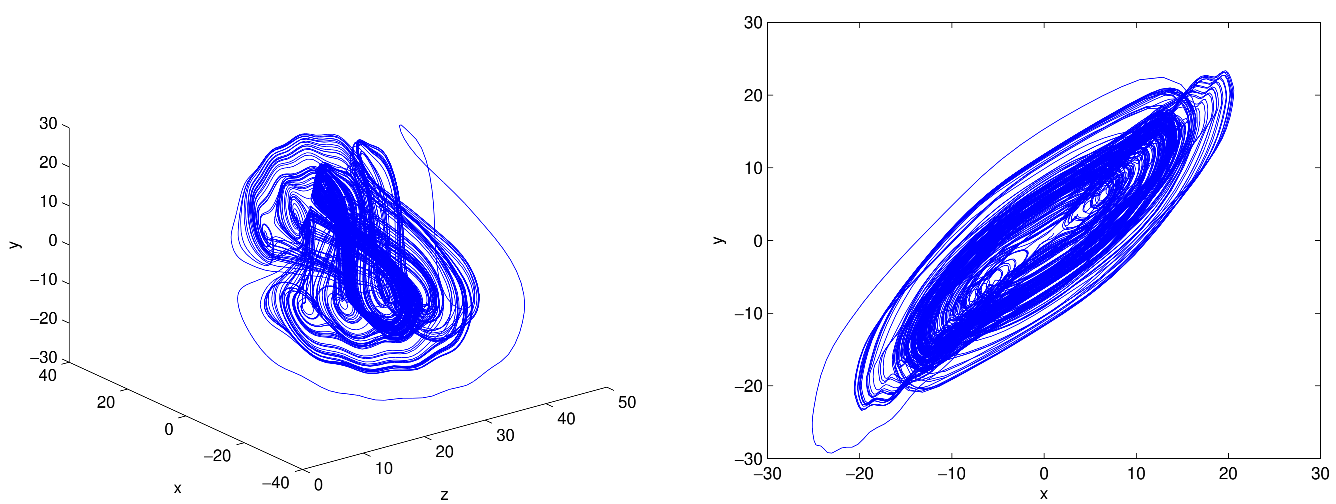

(a) (b)

Fig. 2. The phase portraits of the controlled Chen system. (a) $z - x - y$; (b) $x - y$; (c) $y - z$; (d) $x - z$.

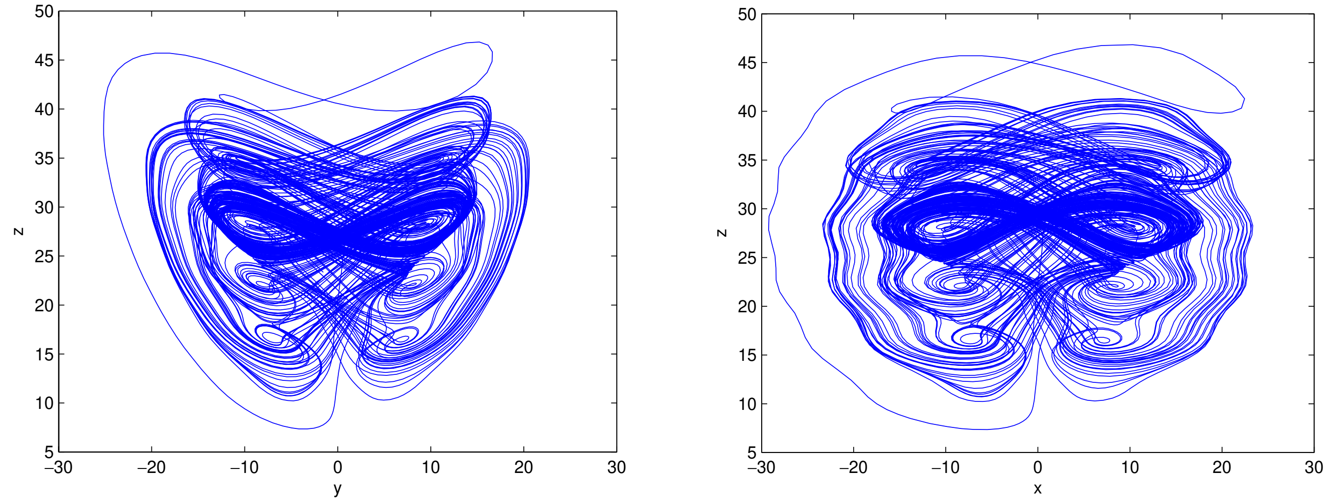

(c) (d)

Fig. 2. (*Continued*)

3. Dynamical Analysis

System (2) has eleven equilibrium points $(0,0,0)$, $(\pm 6.9995, \pm 6.9995, 16.3311)$, $(\pm 7.4572, \pm 7.4572, 18.5365)$, $(\pm 8.1020, \pm 8.1020, 21.8808)$, $(\pm 8.7929, \pm 8.7929, 25.7719)$ and $(\pm 9.0592, \pm 9.0592, 27.3561)$. At the equilibrium point (x^*, y^*, z^*), the characteristic equation of the linearized system is

$$\begin{vmatrix} -a-\lambda & a & 0 \\ c-a-(d_1 z^* - d_2 \sin z^*) & c-\lambda & -d_1 x^* + d_2 x^* \cos z^* \\ y^* & x^* & -b-\lambda \end{vmatrix} = 0 \quad (3)$$

Table 1. List of equilibrium points and corresponding roots of characteristic equations.

No.	Equilibrium Point	Roots of Characteristic Equation	No.	Equilibrium Point	Roots of Characteristic Equation
1	(0, 0, 0)	$\lambda_1 = -30.8359$ $\lambda_2 = -3.0000$ $\lambda_3 = 23.8359$	7	(8.1020, 8.1020, 21.8808)	$\lambda_1 = -31.7110$ $\lambda_2 = 10.8555 + 34.3397i$ $\lambda_3 = 10.8555 - 34.3397i$
2	(−6.9995, −6.9995, 16.3311)	$\lambda_1 = -28.3291$ $\lambda_2 = 9.1646 + 28.6971i$ $\lambda_3 = 9.1646 - 28.6971i$	8	(−8.7929, −8.7929, 25.7719)	$\lambda_1 = -20.8583 + 22.1342i$ $\lambda_2 = -20.8583 - 22.1342i$ $\lambda_3 = 31.7166$
3	(6.9995, 6.9995, 16.3311)	$\lambda_1 = -28.3291$ $\lambda_2 = 9.1646 + 28.6971i$ $\lambda_3 = 9.1646 - 28.6971i$	9	(8.7929, 8.7929, 25.7719)	$\lambda_1 = -20.8583 + 22.1342i$ $\lambda_2 = -20.8583 - 22.1342i$ $\lambda_3 = 31.7166$
4	(−7.4572, −7.4572, 18.5365)	$\lambda_1 = -20.0227 + 21.3456i$ $\lambda_2 = -20.0227 - 21.3456i$ $\lambda_3 = 30.0454$	10	(−9.0592, −9.0592, 27.3561)	$\lambda_1 = -30.2290$ $\lambda_2 = 10.1145 + 31.7952i$ $\lambda_3 = 10.1145 - 31.7952i$
5	(7.4572, 7.4572, 18.5365)	$\lambda_1 = -20.0227 + 21.3456i$ $\lambda_2 = -20.0227 - 21.3456i$ $\lambda_3 = 30.0454$	11	(9.0592, 9.0592, 27.3561)	$\lambda_1 = -30.2290$ $\lambda_2 = 10.1145 + 31.7952i$ $\lambda_3 = 10.1145 - 31.7952i$
6	(−8.1020, −8.1020, 21.8808)	$\lambda_1 = -31.7110$ $\lambda_2 = 10.8555 + 34.3397i$ $\lambda_3 = 10.8555 - 34.3397i$			

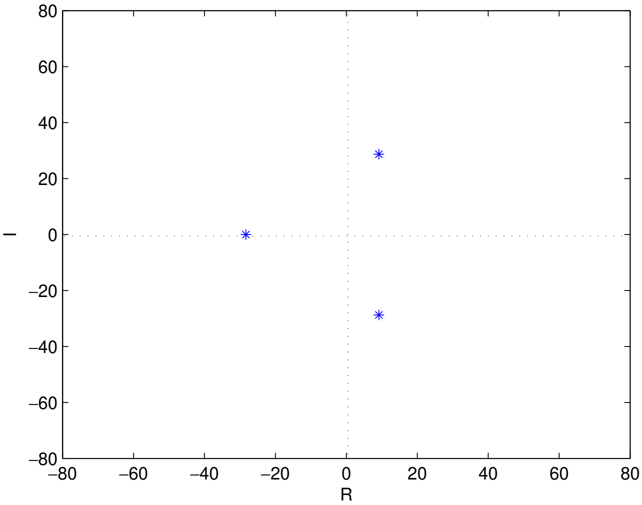

Fig. 3. The roots of the characteristic equations of system (2) corresponding to equilibrium points (±6.9995, $\pm6.9995, 16.3311$).

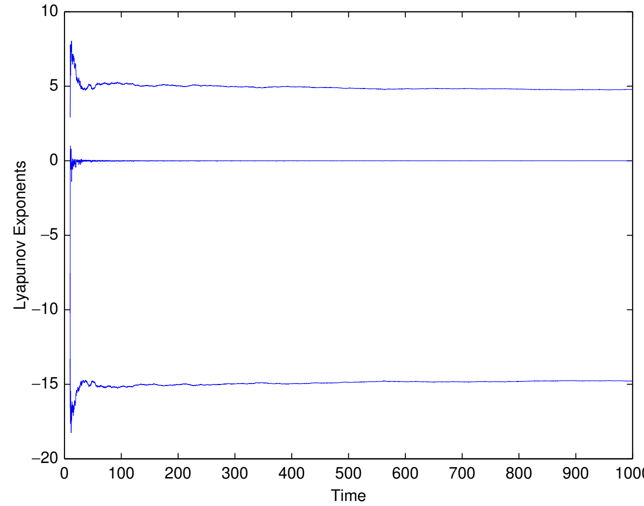

Fig. 4. The Lyapunov spectra of system (2) with $t = 1000$, starting from $(1, 1, 30)$.

All equilibrium points and corresponding roots are shown in Table 1.

From Table 1, we can see that all equilibrium points of system (2) are unstable. Figure 3 shows the responding eigenvalues of points (±6.9995, $\pm6.9995, 16.3311$). A pair of complex conjugate eigenvalues of the linearization around these equilibrium points have crossed the imaginary axis of the complex plane. It can be seen that Hopf bifurcation will occur when suitable parameters are chosen. Similarly, at points $(\pm8.1020, \pm8.1020, 21.8808)$ and $(\pm9.0592, \pm9.0592, 27.3561)$, there exist Hopf bifurcations when suitable parameters are chosen.

Furthermore, we calculate the maximum Lyapunov exponent $\mathrm{LE}_{\max} = 4.7859$ and Lyapunov dimension $d = 2.3236$ using the Matlab LET toolbox. The Lyapunov spectra are shown in Fig. 4.

4. Generalized Multi-Scroll Chaos

From Fig. 2, we can see that the above new chaos is a 6-scroll Chen attractor. Furthermore, by choosing different values of the parameter d_2, we can control the number of equilibrium points of system (2). Subsequently, we can design complex chaotic systems with different topological structures by controlling the number of Hopf bifurcation points.

When $d_2 = 5$, system (2) has seven equilibrium points $(0, 0, 0)$, $(\pm7.0847, \pm7.0847, 16.7311)$, $(\pm7.4039, \pm7.4039, 18.2726)$ and $(\pm8.0917, \pm8.0917, 21.8253)$. At points $(\pm7.0847, \pm7.0847, 16.7311)$ and $(\pm8.0917, \pm8.0917, 21.8253)$, there exist Hopf bifurcations when suitable parameters are chosen. Figure 5 shows the phase portraits of state variables of system (2) with $d_2 = 5$, which is a 4-scroll attractor. The maximum Lyapunov exponent is $\mathrm{LE}_{\max} = 0.4015$ and Lyapunov dimension $d = 2.0316$.

When $d_2 = 14$, system (2) has 19 equilibrium points

$$(0, 0, 0), (\pm5.5575, \pm5.5575, 10.2952), (\pm5.9635, \pm5.9635, 11.8545), (\pm6.9429, \pm6.9429, 16.0680),$$
$$(\pm7.4867, \pm7.4867, 18.6833), (\pm8.1102, \pm8.1102, 21.9250), (\pm8.7390, \pm8.7390, 25.4567),$$
$$(\pm9.1274, \pm9.1274, 27.7696), (\pm9.8534, \pm9.8534, 32.3629) \text{ and } (\pm10.0190, \pm10.0190, 33.4602).$$

At points

$$(\pm5.5575, \pm5.5575, 10.2952), (\pm6.9429, \pm6.9429, 16.0680), (\pm8.1102, \pm8.1102, 21.9250),$$
$$(\pm9.1274, \pm9.1274, 27.7696) \text{ and } (\pm10.0190, \pm10.0190, 33.4602),$$

there exist Hopf bifurcations when suitable parameters are chosen. Figure 6 shows the phase portraits of state variables of system (2) with $d_2 = 14$, which is a 10-scroll attractor. The maximum Lyapunov exponent is $\mathrm{LE}_{\max} = 7.0722$ and Lyapunov dimension $d = 2.4142$.

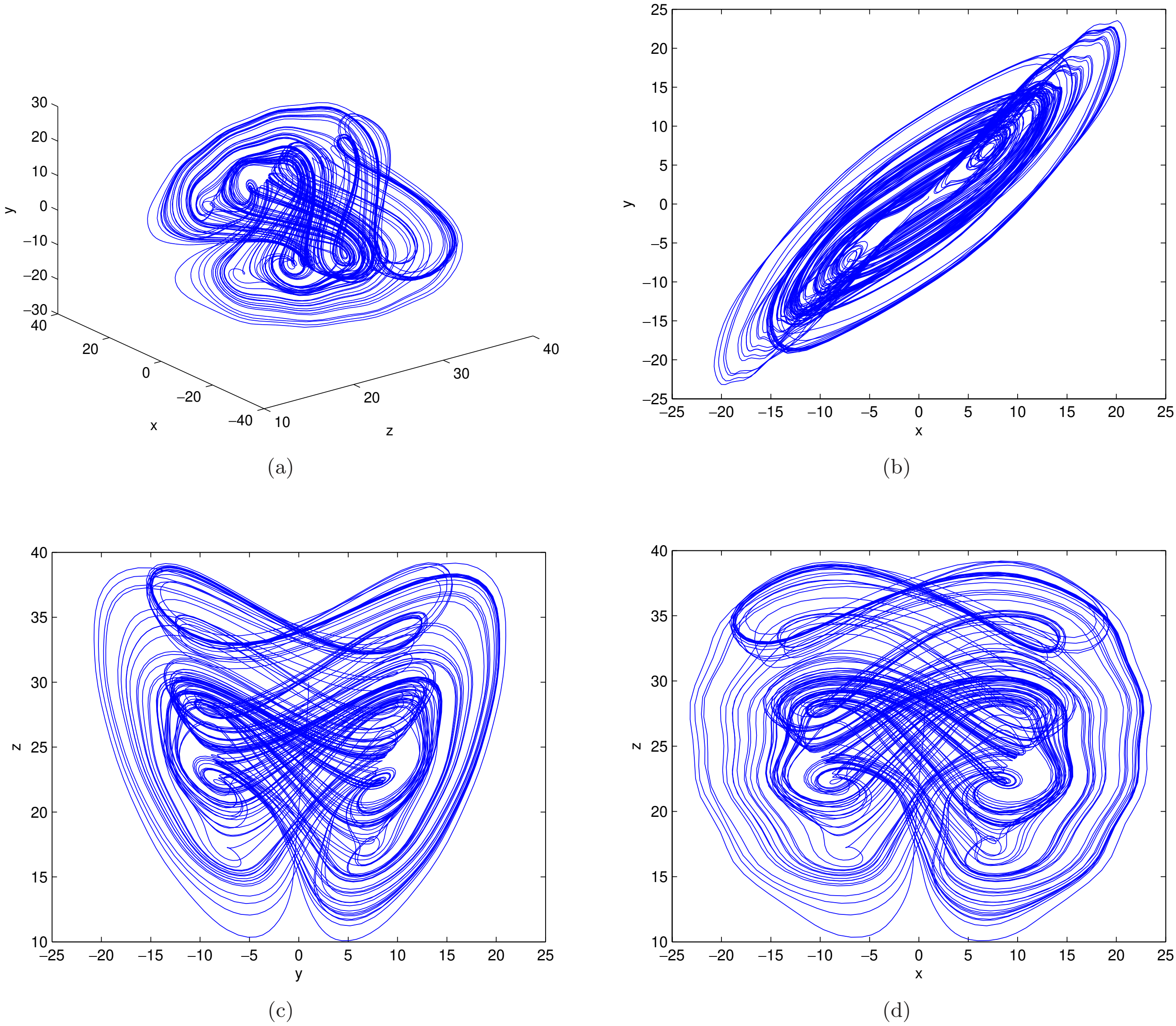

Fig. 5. The phase portraits of system (2) with $d_2 = 5$, starting from $(1, 1, 30)$. (a) $z - x - y$; (b) $x - y$; (c) $y - z$; (d) $x - z$.

When $d_2 = 22$, system (2) has 27 equilibrium points

$$(0, 0, 0), (\pm 3.4741, \pm 3.4741, 4.0231), (\pm 4.0626, \pm 4.0626, 5.5015), (\pm 5.4638, \pm 5.4638, 9.9510),$$
$$(\pm 6.0380, \pm 6.0380, 12.1525), (\pm 6.9152, \pm 6.9152, 15.9400), (\pm 7.4994, \pm 7.4994, 18.7470),$$
$$(\pm 8.1144, \pm 8.1144, 21.9480), (\pm 8.7174, \pm 8.7174, 25.3309), (\pm 9.1574, \pm 9.1574, 27.9528),$$
$$(\pm 9.7882, \pm 9.7882, 31.9362), (\pm 10.0890, \pm 10.0890, 33.9293), (\pm 10.7650, \pm 10.7650, 38.6286)$$
$$\text{and } (\pm 10.9291, \pm 10.9291, 39.8147).$$

At points

$$(\pm 3.4741, \pm 3.4741, 4.0231), (\pm 5.4638, \pm 5.4638, 9.9510), (\pm 6.9152, \pm 6.9152, 15.9400),$$
$$(\pm 8.1144, \pm 8.1144, 21.9480), (\pm 9.1574, \pm 9.1574, 27.9528), (\pm 10.0890, \pm 10.0890, 33.9293)$$
$$\text{and } (\pm 10.9291, \pm 10.9291, 39.8147),$$

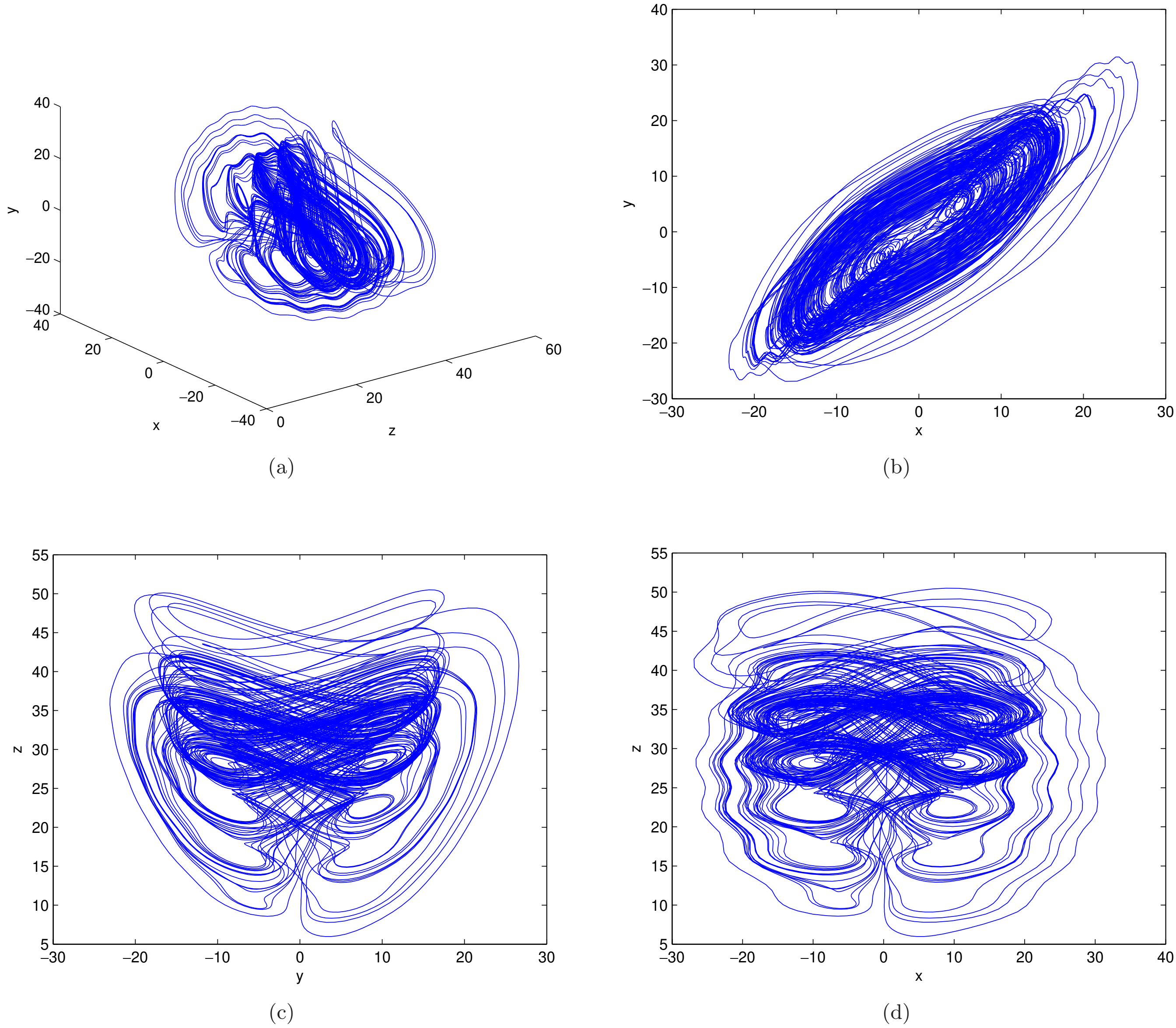

Fig. 6. The phase portraits of system (2) with $d_2 = 14$, starting from $(1, 1, 30)$. (a) $z - x - y$; (b) $x - y$; (c) $y - z$; (d) $x - z$.

there exist Hopf bifurcations when suitable parameters are chosen. Figure 7 shows the phase portraits of state variables of system (2) with $d_2 = 22$, which is a 14-scroll attractor. The maximum Lyapunov exponent is $\mathrm{LE}_{\max} = 8.6318$ and Lyapunov dimension $d = 2.4632$.

When $d_2 = 28$, system (2) has 31 equilibrium points

$$\begin{aligned}
&(0,0,0), (\pm 3.3777, \pm 3.3777, 3.8029), (\pm 4.1371, \pm 4.1371, 5.7053), (\pm 5.4318, \pm 5.4318, 9.8349),\\
&(\pm 6.0618, \pm 6.0618, 12.2485), (\pm 6.9047, \pm 6.9047, 15.8914), (\pm 7.5040, \pm 7.5040, 18.7698),\\
&(\pm 8.1161, \pm 8.1161, 21.9570), (\pm 8.7097, \pm 8.7097, 25.2864), (\pm 9.1686, \pm 9.1686, 28.0209),\\
&(\pm 9.7692, \pm 9.7692, 31.8124), (\pm 10.1102, \pm 10.1102, 34.0718), (\pm 10.7287, \pm 10.7287, 38.3682),\\
&(\pm 10.9668, \pm 10.9668, 40.0905), (\pm 11.6206, \pm 11.6206, 45.0129)\\
&\text{and } (\pm 11.7497, \pm 11.7497, 46.0188).
\end{aligned}$$

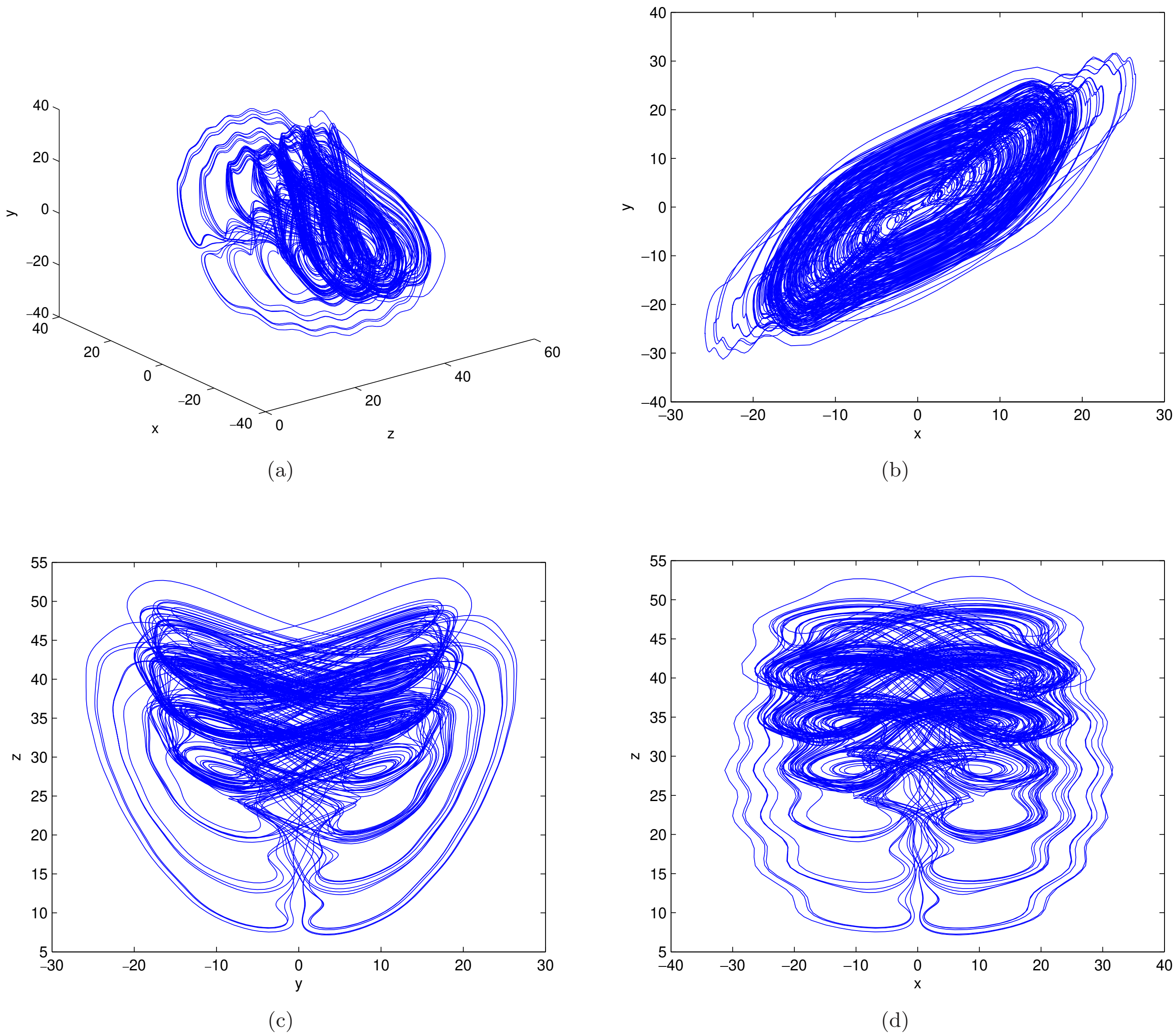

Fig. 7. The phase portraits of system (2) with $d_2 = 22$, starting from $(1, 1, 30)$. (a) $z - x - y$; (b) $x - y$; (c) $y - z$; (d) $x - z$.

At points

$$(\pm 3.3777, \pm 3.3777, 3.8029), (\pm 5.4318, \pm 5.4318, 9.8349), (\pm 6.9047, \pm 6.9047, 15.8914),$$
$$(\pm 8.1161, \pm 8.1161, 21.9570), (\pm 9.1686, \pm 9.1686, 28.0209), (\pm 10.1102, \pm 10.1102, 34.0718),$$
$$(\pm 10.9668, \pm 10.9668, 40.0905) \text{ and } (\pm 11.7497, \pm 11.7497, 46.0188),$$

there exist Hopf bifurcations when suitable parameters are chosen. Figure 8 shows the phase portraits of state variables of system (2) with $d_2 = 28$, which is a 16-scroll attractor. The maximum Lyapunov exponent is $\mathrm{LE}_{\max} = 8.7869$ and Lyapunov dimension $d = 2.4677$.

Figure 9 shows that all three Lyapunov exponents change as d_2 ranges in $[5, 20]$ with fixed parameters $a = 35, b = 3, c = 28$ and $d_1 = 1$.

Remark. When parameter d_2 increases, the number of equilibrium points increases correspondingly.

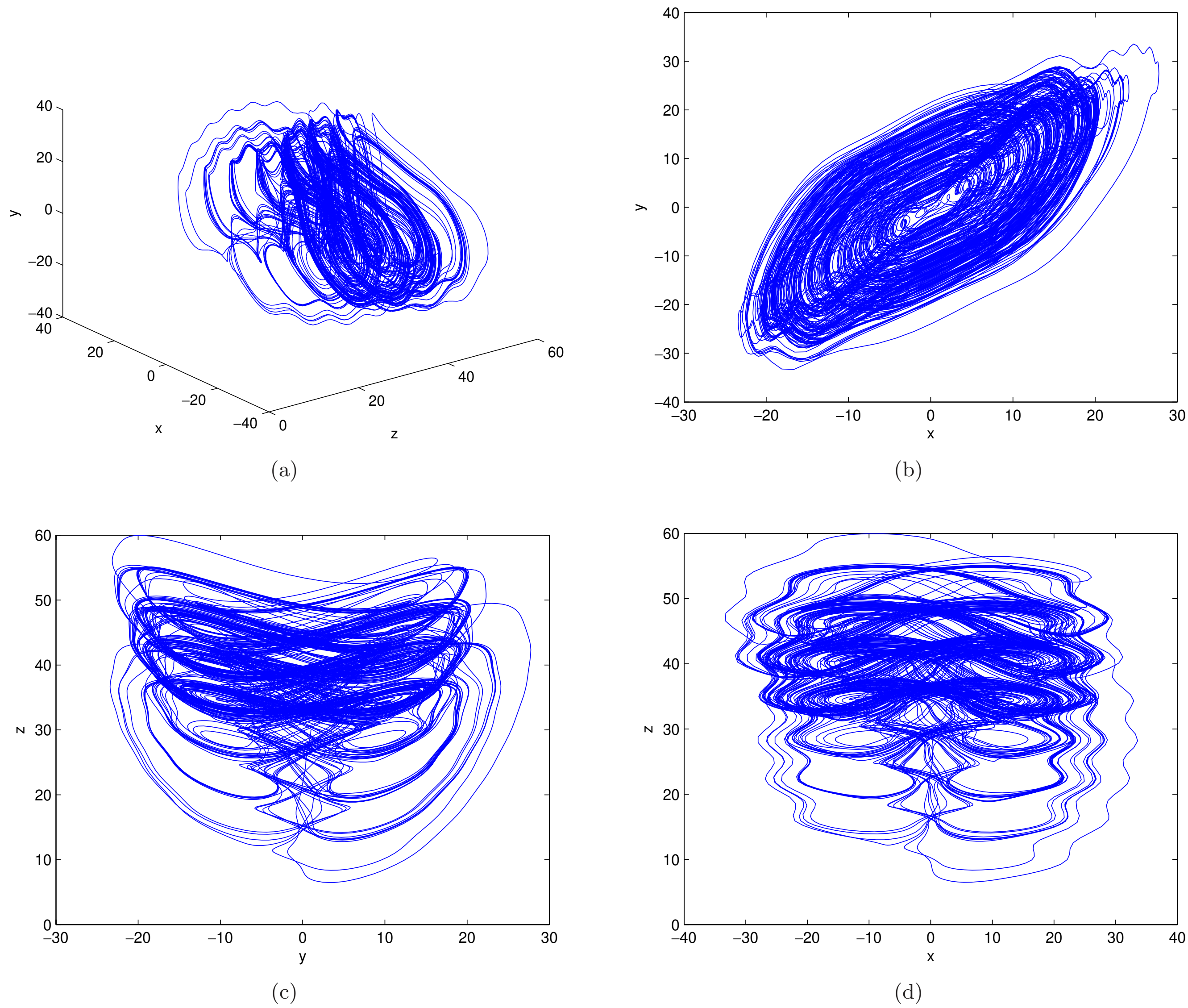

Fig. 8. The phase portraits of system (2) with $d_2 = 28$, starting from $(1, 1, 30)$. (a) $z - x - y$; (b) $x - y$; (c) $y - z$; (d) $x - z$.

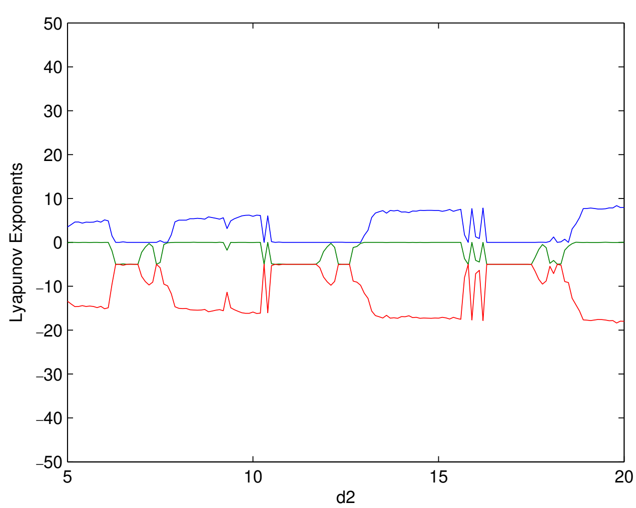

Fig. 9. All Lyapunov exponents versus parameter d_2 in $[5, 20]$ with $a = 35, b = 3, c = 28$ and $d_1 = 1$.

With Hopf bifurcation occurring over and over again, system (2) generates new attractors with more scrolls.

5. Generalized Complex Chaos and Hyperchaos

It is well known that first-order delay differential equation can generate hyperchaotic dynamic behavior. In order to generalize system (2) to more complex chaos and hyperchaos, we introduce time delay to control function, $u(t) = d_0 z(t) + d_1 z(t-\tau) - d_2 \sin(z(t-\tau))$. System (2) transforms to the following.

$$\begin{cases} \dot{x} = a(y-x) \\ \dot{y} = (c-a)x - x(d_0 z(t) + d_1 z(t-\tau) \\ \qquad - d_2 \sin(z(t-\tau))) + cy \\ \dot{z} = xy - bz \end{cases} \tag{4}$$

where d_0, d_1, d_2 are constants and τ is the time delay. When suitable parameters are chosen, system (4) can generate complex chaotic and hyperchaotic attractors as follows.

5.1. *Special case I*: $d_0 = d_1$

(i) When $d_0 = 1$, $d_1 = 1$, $d_2 = 5$ and $\tau = 0.2$, system (4) generates complex chaotic dynamic behaviors (shown in Fig. 10).

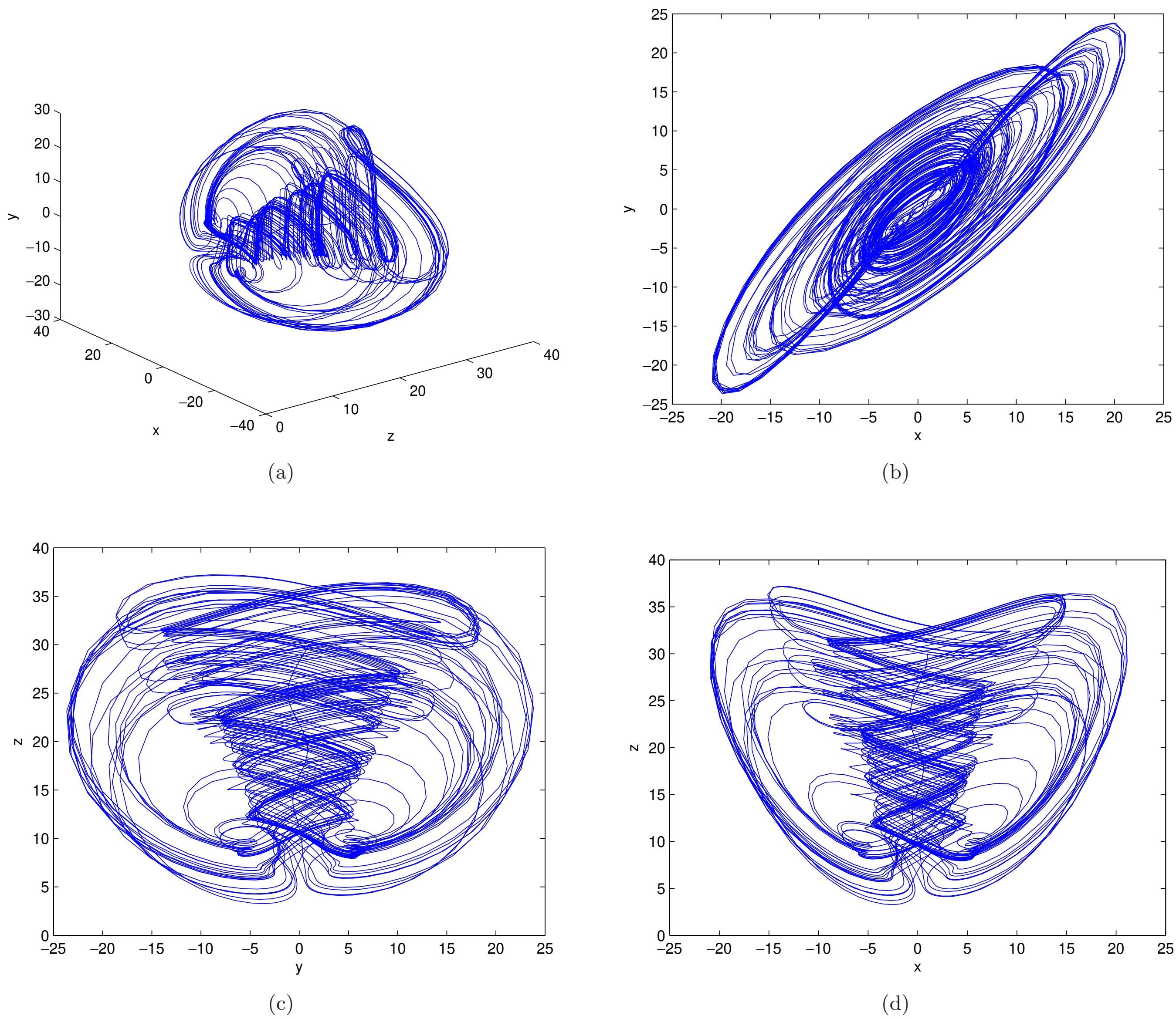

Fig. 10. The phase portraits of system (4) with $d_0 = 1, d_1 = 1, d_2 = 5$ and $\tau = 0.2$.

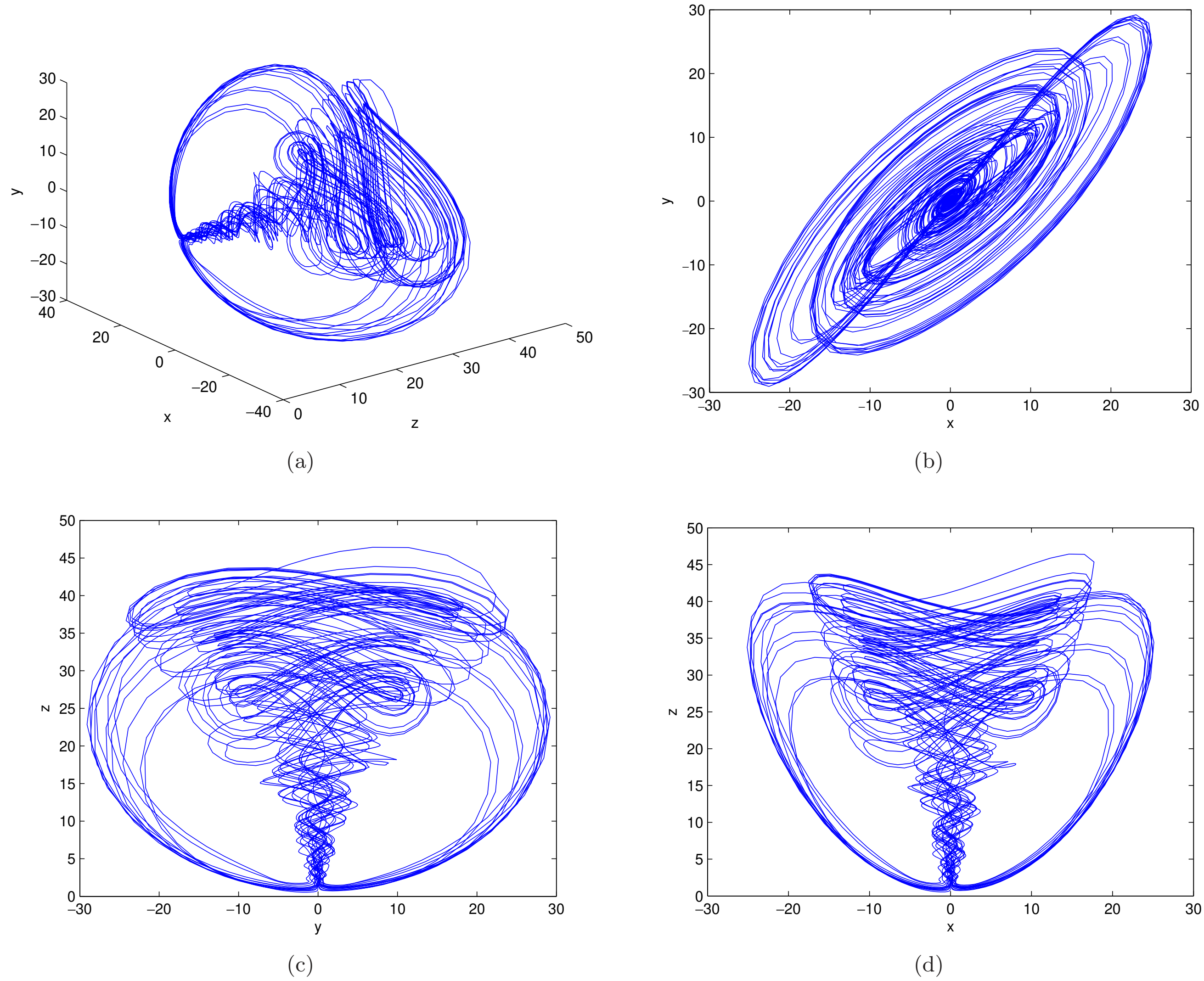

Fig. 11. The phase portraits of system (4) with $d_0 = 1, d_1 = 1, d_2 = 5$ and $\tau = 0.8$.

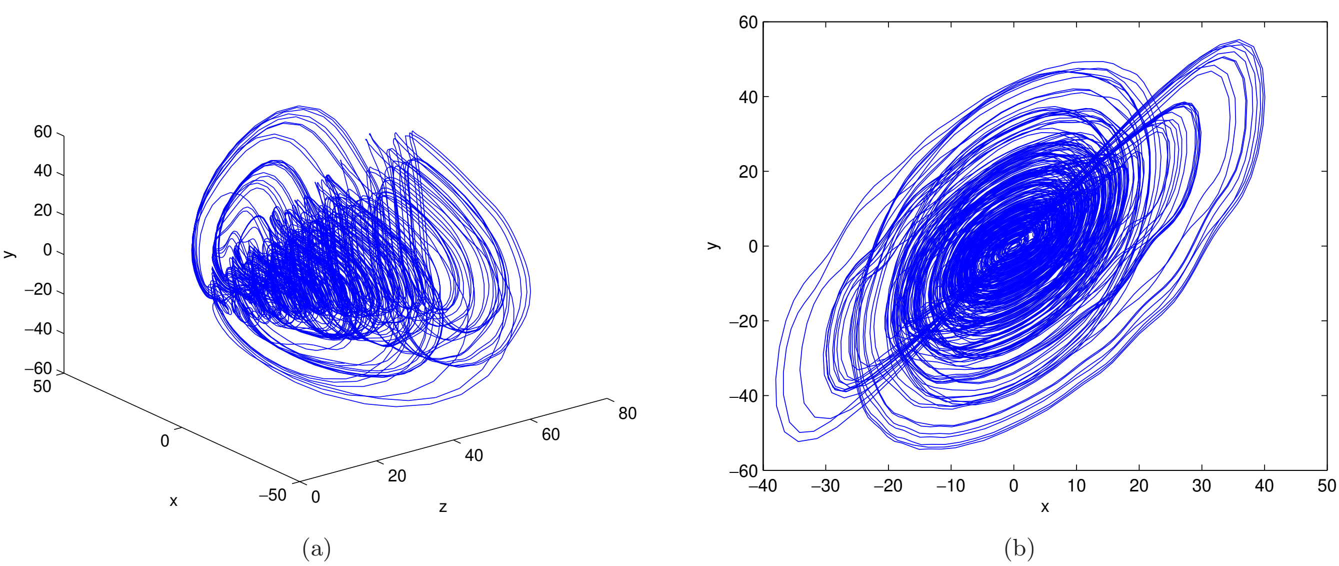

Fig. 12. The phase portraits of system (4) with $d_0 = 1, d_1 = 1, d_2 = 30$ and $\tau = 0.05$.

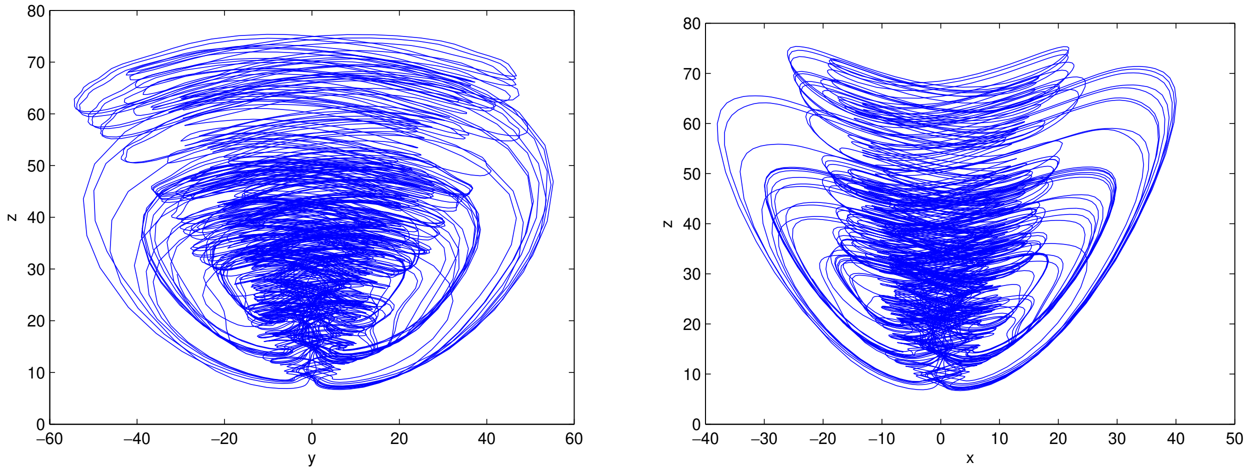

(c) (d)

Fig. 12. (*Continued*)

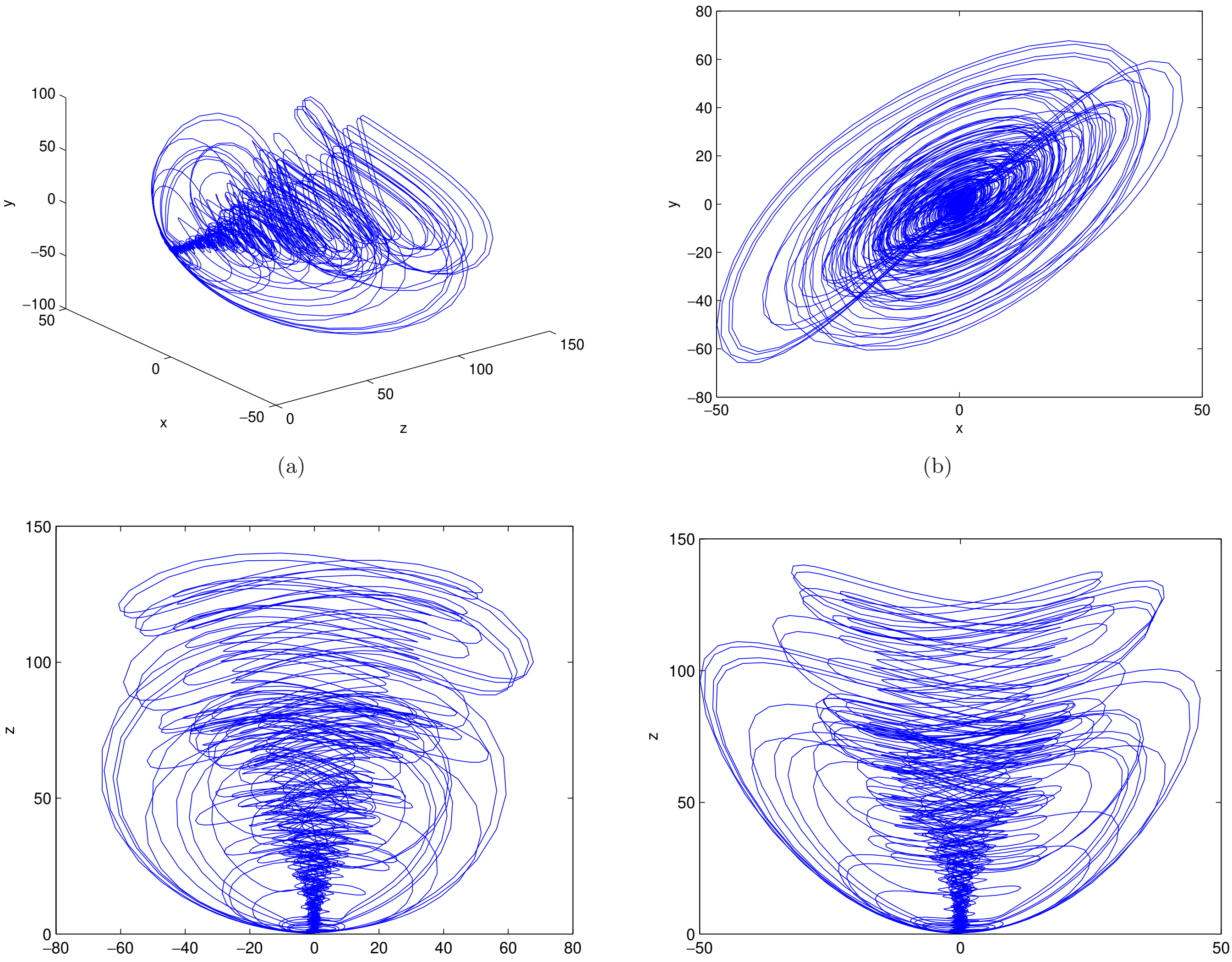

(a) (b) (c) (d)

Fig. 13. The phase portraits of system (4) with $d_0 = 1, d_1 = 1, d_2 = 30$ and $\tau = 0.8$.

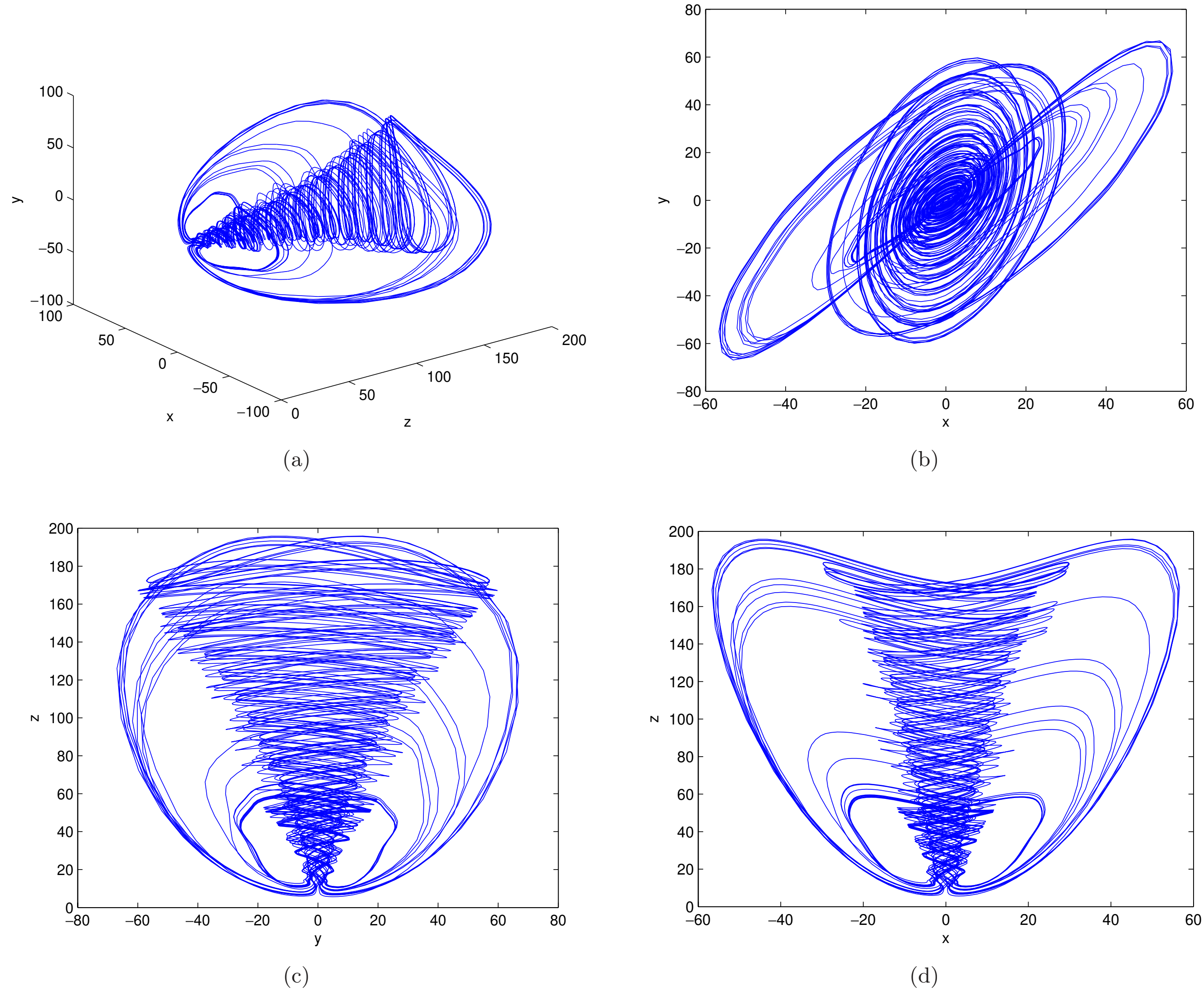

Fig. 14. The phase portraits of system (4) with $d_0 = 0.2, d_1 = 1, d_2 = 5$ and $\tau = 0.1$.

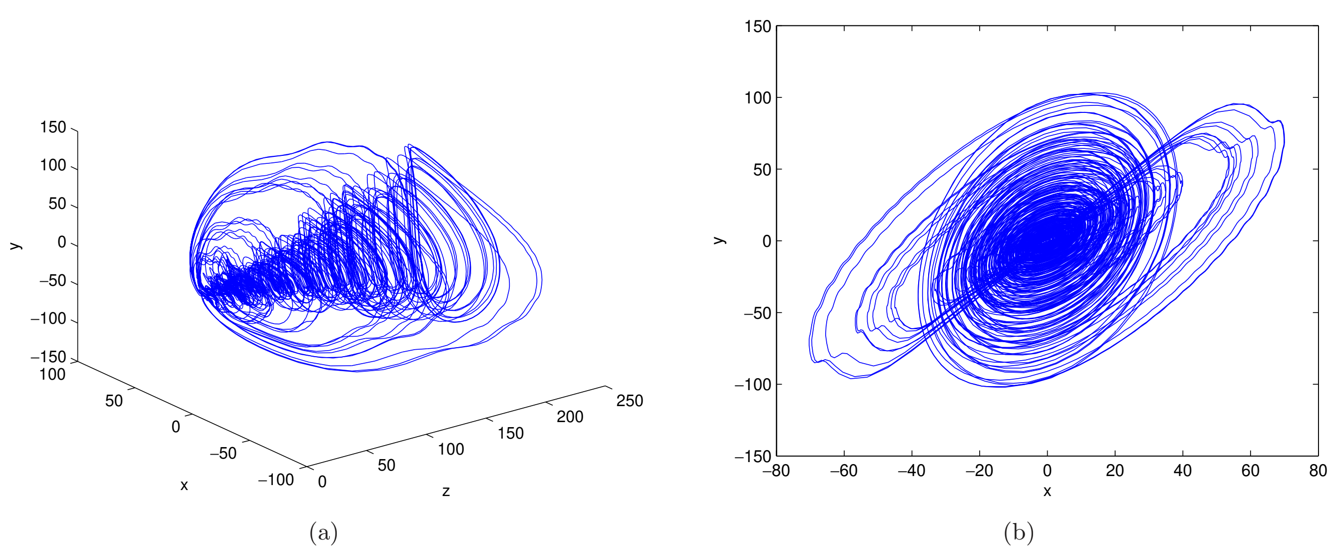

Fig. 15. The phase portraits of system (4) with $d_0 = 0.2, d_1 = 1, d_2 = 30$ and $\tau = 0.05$.

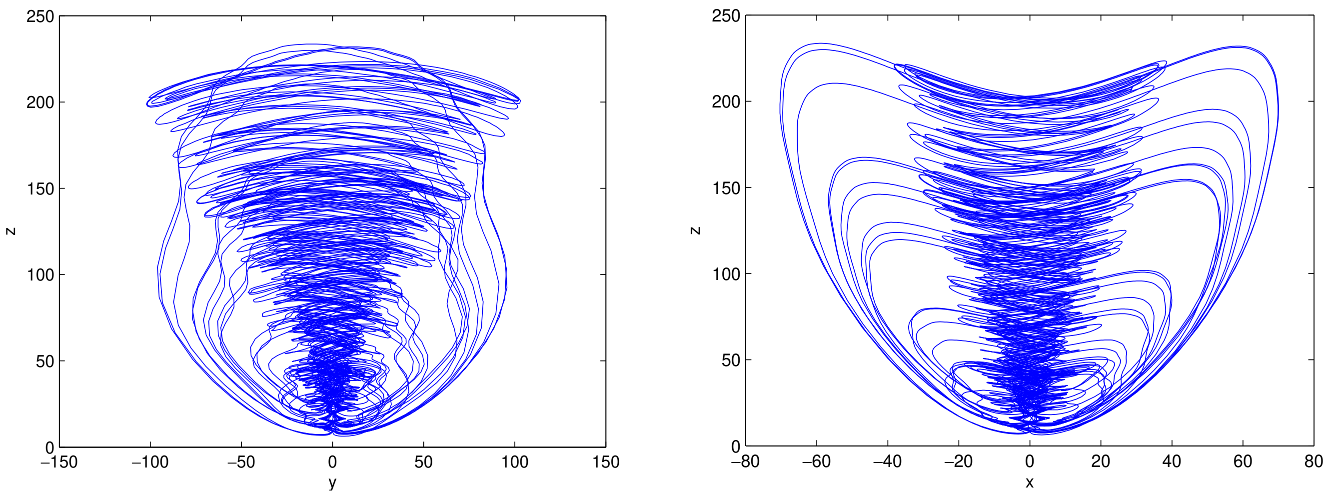

(c) (d)

Fig. 15. (*Continued*)

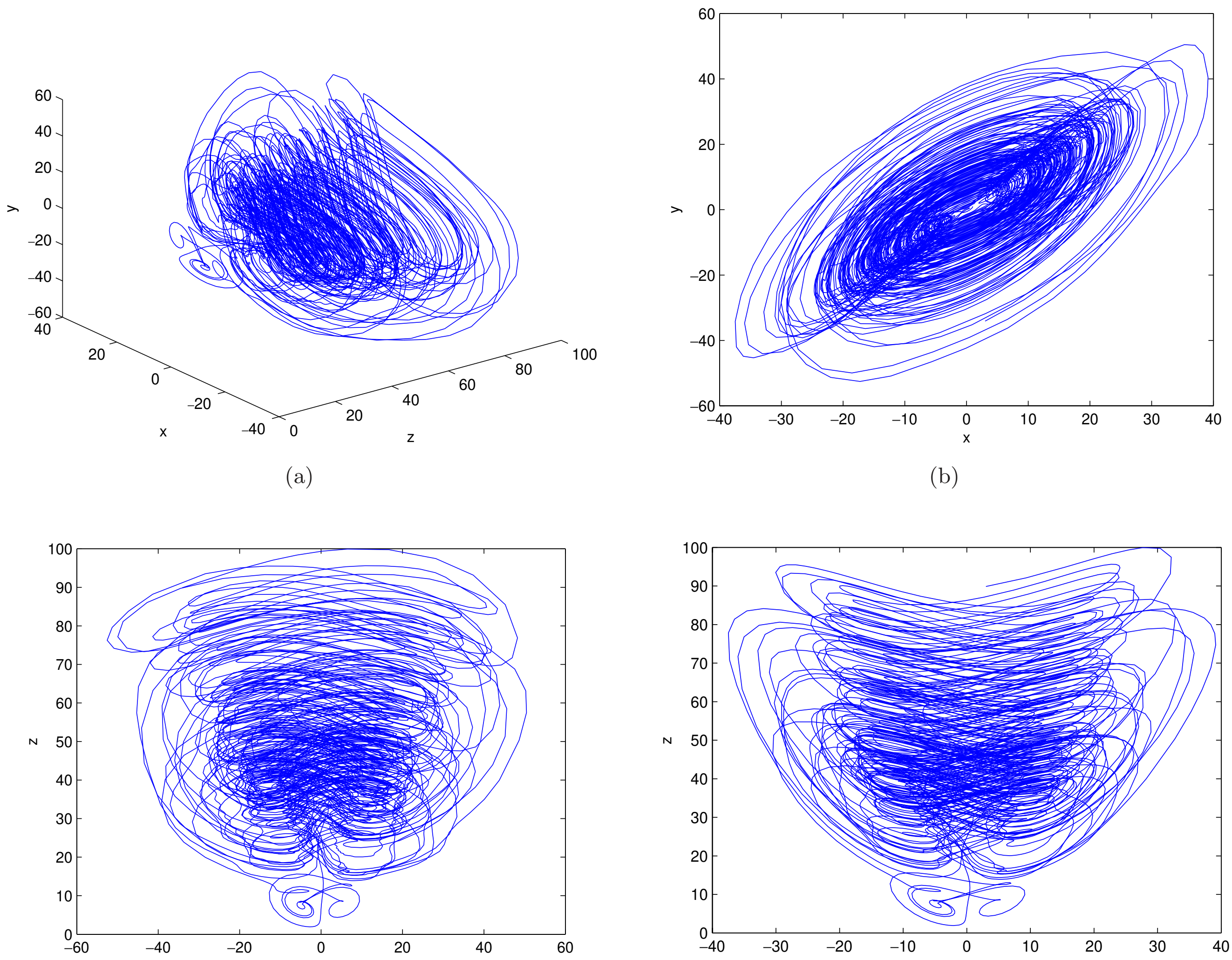

(a) (b)

(c) (d)

Fig. 16. The phase portraits of system (4) with $d_0 = 1, d_1 = -0.2, d_2 = 20$ and $\tau = 5$.

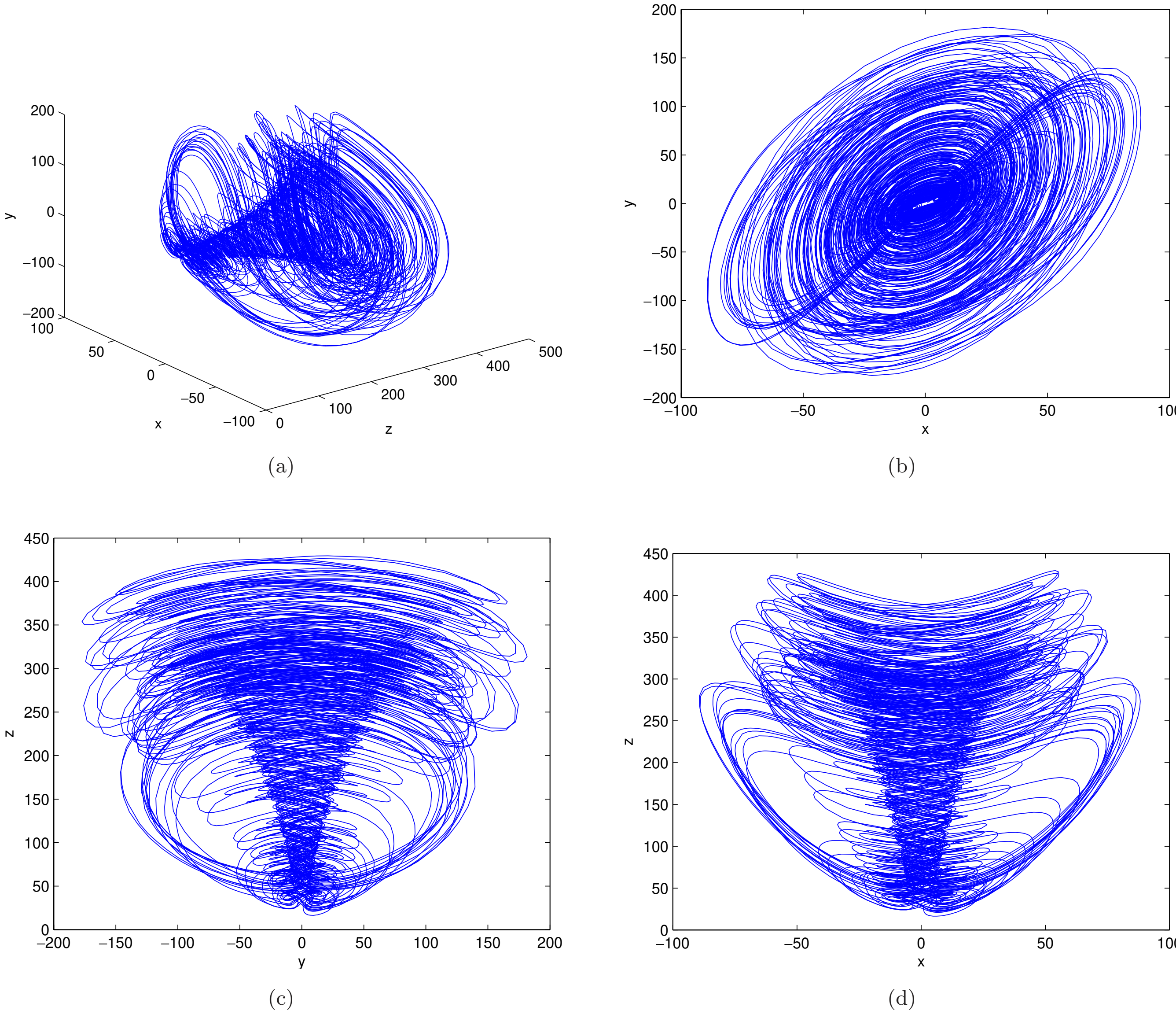

Fig. 17. The phase portraits of system (4) with $d_0 = 1, d_1 = -0.4, d_2 = 5$ and $\tau = 1$.

(ii) When $d_0 = 1$, $d_1 = 1$, $d_2 = 5$ and $\tau = 0.8$, system (4) generates complex chaotic dynamic behaviors (shown in Fig. 11).

(iii) When $d_0 = 1$, $d_1 = 1$, $d_2 = 30$ and $\tau = 0.05$, system (4) generates complex chaotic dynamic behaviors (shown in Fig. 12).

(iv) When $d_0 = 1$, $d_1 = 1$, $d_2 = 30$ and $\tau = 0.8$, system (4) generates complex chaotic dynamic behaviors (shown in Fig. 13).

5.2. *Special case II*: $d_0 \neq d_1$

(i) When $d_0 = 0.2, d_1 = 1, d_2 = 5$ and $\tau = 0.1$, system (4) generates complex chaotic dynamic behaviors (shown in Fig. 14).

(ii) When $d_0 = 0.2$, $d_1 = 1$, $d_2 = 30$ and $\tau = 0.05$, system (4) generates complex chaotic dynamic behaviors (shown in Fig. 15).

(iii) When $d_0 = 1, d_1 = -0.2, d_2 = 20$ and $\tau = 5$, system (4) generates complex chaotic dynamic behaviors (shown in Fig. 16).

(iv) When $d_0 = 1, d_1 = -0.4, d_2 = 5$ and $\tau = 1$, system (4) generates complex chaotic dynamic behaviors (shown in Fig. 17).

6. Conclusion

We have presented a feedback control function to generate multi-scroll attractors from the Chen system. Then we have analyzed the dynamical behavior of this new attractor. By varying the control parameters, we have achieved a set of new attractors with different scrolls. After that, we have generalized the multi-scroll attractors to generate more complex chaos and hyperchaos by introducing time delay to the control function. This kind of control method may also be used to other chaotic systems.

References

Ahmad, W. M. & Sprott, J. C. [2003] "Chaos in fractional-order autonomous nonlinear systems," *Chaos Solit. Fract.* **16**, 339–351.

Ballinger, G. & Liu, X. [1997] "On boundedness of solutions of impulsive systems," *Nonlin. Stud.* **4**, 121–131.

Chen, G. & Ueta, T. [1999] "Yet another chaotic attractor," *Int. J. Bifurcation and Chaos* **9**, 1465–1466.

Chua, L. O., Wu, C. W., Huang, A. & Zhong, G. [1993] "A universal circuit for studying and generating chaos. I. Routes to chaos," *IEEE Trans. Circuits Syst.-I* **40**, 732–744.

Cuomo, K. M. & Oppenheim, A. V. [1993] "Circuit implementation of synchronized chaos with applications to communications," *Phys. Rev. Lett.* **71**, 65–68.

Elwakil, A. S. & Kennedy, M. P. [2001] "Construction of classes of circuit-independent chaotic oscillatorsusing passive-only nonlinear devices," *IEEE Trans. Circuits Syst.-I* **48**, 289–307.

Elwakil, A. S. & Ozoguz, S. [2006] "Multi-scroll chaotic oscillators: The nonautonomous approach," *IEEE Trans. Circuits Syst.-II* **53**, 862–866.

Farmer, J. [1982] "Chaotic attractors of an infinite-dimensional dynamical system," *Physica D* **4**, 366–393.

Goedgebuer, J., Larger, L. & Porte, H. [1998] "Optical cryptosystem based on synchronization of hyperchaos generated by a delayed feedback tunable laser diode," *Phys. Rev. Lett.* **80**, 2249–2252.

Grassi, G. & Mascolo, S. [1999] "Synchronizing hyperchaotic systems by observer design," *IEEE Trans. Circuits Syst.-II* **46**, 478–483.

Hartley, T., Lorenzo, C. & Qammer, H. K. [1995] "Chaos in a fractional order Chua's system," *IEEE Trans. Circuits Syst.-I* **42**, 485–490.

Ikeda, K. & Matsumoto, K. [1987] "High-dimensional chaotic behavior in systems with time-delayed feedback," *Physica D* **29**, 223–235.

Khadra, A., Liu, X. & Shen, X. [2003] "Application of impulsive synchronization to communication security," *IEEE Trans. Circuits Syst.-I* **50**, 341–351.

Kocarev, L., Halle, K. S., Eckert, K., Chua, L. O. & Parlitz, U. [1992] "Experimental demonstration of secure communications via chaotic synchronization," *Int. J. Bifurcation and Chaos* **2**, 709–713.

Li, C. & Chen, G. [2004] "Chaos and hyperchaos in the fractional-order Rossler equations," *Physica A* **341**, 55–61.

Li, Y., Liu, X. & Zhang, H. [2005] "Dynamical analysis and impulsive control of a new hyperchaotic system," *Math. Comput. Model.* **42**, 1359–1374.

Liu, X. [2006] "Stability of linear delay systems via impulsive control," *Int. J. Dyn. Contin. Discr. Impul. Syst.* **13**, 791–803.

Liu, X., Teo, K. L., Zhang, H. & Chen, G. [2006] "Switching control of linear systems for generating chaos," *Chaos Solit. Fract.* **30**, 725–733.

Lu, H. & He, Z. [1996] "Chaotic behavior in first-order autonomous continuous-time systems with delay," *IEEE Trans. Circuits Syst.-I* **43**, 700–702.

Lu, J., Han, F., Yu, X. & Chen, G. [2004] "Generating 3-D multi-scroll chaotic attractors: A hysteresis series switching method," *Automatica* **40**, 1677–1687.

Namajunas, A., Pyragas, K. & Tamasevicius, A. [1995] "An electronic analog of the Mackey–Glass system," *Phys. Lett. A* **201**, 42–46.

Pecora, L. M. & Carroll, T. L. [1990] "Synchronization in chaotic systems," *Phys. Rev. Lett.* **64**, 821–824.

Peng, J. H., Ding, E. J., Ding, M. & Yang, W. [1996] "Synchronizing hyperchaos with a scalar transmitted signal," *Phys. Rev. Lett.* **76**, 904–907.

Rossler, O. E. [1979] "An equation for hyperchaos," *Phys. Lett. A* **71**, 155–157.

Tamasevicius, A., Mykolaitis, G. & Bumeliene, S. [2006] "Delayed feedback chaotic oscillator with improved spectral characteristics," *Electron. Lett.* **42**, 736–737.

Wang, L. & Yang, X. [2006] "Generation of multi-scroll delayed chaotic oscillator," *Electron. Lett.* **42**, 1439–1441.

Yalcin, M., Suykens, J., Vandewalle, J. & Ozoguz, S. [2002] "Families of scroll grid attractors," *Int. J. Bifurcation and Chaos* **12**, 23–41.

Yalcin, M. [2007] "Multi-scroll and hypercube attractors from a general jerk circuit using Josephson junctions," *Chaos Solit. Fract.* **34**, 1659–1666.

Yalcin, M. & Ozoguz, S. [2007] "N-scroll chaotic attractors from a first-order time-delay differential equation," *Chaos* **17**, 033112.

Yan, Z. Y. & Yu, P. [2008] "Hyperchaos synchronization and control on a new hyperchaotic attractor," *Chaos Solit. Fract.* **35**, 333–345.

Yang, T. & Chua, L. O. [1996] "Ecure communication via chaotic parameter modulation," *IEEE Trans. Circuits Syst.-I* **43**, 817–819.